Temperature-Dependent Properties of Water-in-Oil Microemulsions with Amphiphilic Triblock-Copolymer. Part I: Dynamics, Particle Interactions, and Network Formation

Holger Mays* and Mats Almgren

Department of Physical Chemistry, University of Uppsala, Box 532, S-751 21 Uppsala, Sweden

Received: March 26, 1999

The properties of pseudo-ternary mixtures of *p*-xylene with the amphiphilic triblock-copolymer $PEO_{13}PPO_{30}PEO_{13}$ (Pluronic L64) and water in the L_2-phase (water-in-oil microemulsions) are examined. The applied experimental methods are electric conductivity, time-resolved luminescence quenching (TRLQ), dynamic light scattering (DLS), and rheology. Only the microemulsion with the largest water mass fraction, close to maximum solubilization, exhibits a percolation transition of the electric conductivity when decreasing the temperature. Luminescence quenching and light scattering results prove that the reverse micelle structure is maintained in the highly conducting state. Time-resolved luminescence quenching shows that on the submicrosecond and millisecond time-scale different exchange processes occur. The fast exchange is attributed to intracluster processes. Their rate increases with increasing water content and decreasing temperature, while the inter-cluster exchange remains very slow. At the lowest water mass fraction a temperature decrease leads to a slower exchange. The relaxation time distribution functions obtained from dynamic light scattering show in the entire investigated temperature and water concentration range three diffusive relaxation modes, which stem from unimers, water-swollen reverse micelles and clusters. The cluster size increases with the water content and decreasing temperature and reaches a time-averaged size with the onset of percolation. Static low shear viscosity measurements show a strong increase of the microemulsion viscosity and also a pseudoplastic behavior when lowering the temperature, while no indications for viscoelastic properties are found. The experimental findings are discussed in a self-consistent picture of exothermic and gradual network built-up where reverse micelle linking occurs via the two hydrophilic moieties of the triblock-copolymer molecules. The cluster lifetime, solute migration mechanism and the role of water for the reverse micelle interior are considered. Important and obvious differences of L_2-microemulsions with amphiphilic triblock-copolymer to those with short-chained surfactants are elucidated, and the necessity of applying a variety of methods for achieving an understanding of the complex liquids is emphasized.

Introduction

Amphiphilic triblock-copolymers of the $EO_aPO_bEO_a$-type (EO: ethylene oxide, PO: propylene oxide) have attracted much scientific interest in the past decade, due to theoretical questions concerning the self-assembly of copolymers,[1,2] and their importance in technical applications.[3] Because of their low toxicity and high biodegradability, these substances are widely used as emulsifiers and gelling agents in, for example, food processing, pharmaceutical and cosmetic products, as well as in agricultural formulations.[3−8] Further applications are emulsion stabilization in polymerization reactions,[9] nanomaterial synthesis,[10,11] and coal processing.[12]

Significant for the usage of amphiphilic copolymers is their ability to self-assemble in solution or at interfaces under appropriate conditions and to interact with substrates of different polarity in a different manner. The amphiphilicity is directly reflected in the affinity of the polymer blocks toward different solvents. For instance, water at not too high temperatures is a good solvent for ethylene oxide chains but a poor solvent for polypropylene oxide, polybutylene oxide, or polystyrene chains.[3,13,14] Conversely, organic solvents solubilize well polypropylene oxide but not equally well poly(ethylene oxide). It is this molecular "schizophrenia" leading to the associative and self-assembling properties of amphiphiles in solution.

* Corresponding author. E-mail: Holger.Mays@fki.uu.se.

These properties and related phenomena have received an intense research activity, providing numerous published studies. These include binary systems such as hydrophobically end-capped poly(ethylene oxide)s in water,[15,16] micelles from dissolved surfactants,[17,18] vesicles in water or oil,[19,20] telechelic ionomers in apolar solvents,[21] and di- or triblock-copolymers in solution.[22−24] More complex systems are ternary mixtures, for instance hydrophobically end-capped poly(ethylene oxide)s in water mixed with hydrophilic polymers,[16] or mixtures of water, apolar solvent, and surfactant or triblock-copolymer, mixtures which form microemulsions.[25−30]

The colloidal properties of triblock-copolymer aggregates in aqueous solution and their gelling behavior are relatively well understood,[24,31] for a review see ref 22. Recently, research has been extended to the systematic isothermal investigation of various triblock-copolymers in mixture with water and organic solvent. In such ternary systems, a rich variety of phases with different internal structure was found.[29,30] The triblock-copolymer $EO_{13}PO_{30}EO_{13}$, technically produced and distributed under the trade names Pluronic L64 and Synperonic L64, forms isotropic microemulsion phases with a droplet structure (oil-in-water microemulsion, L_1-phase, respective water-in-oil microemulsion, L_2-phase) as well as a bicontinuous phase (V_2). Also a variety of lyotropic liquid crystals is present in the Gibbs-phase triangle at 25 °C, with a lamellar phase (L_α) and rodlike

10.1021/jp991047d CCC: $18.00 © 1999 American Chemical Society
Published on Web 10/06/1999

micelles or reverse micelles ordered in an hexagonal lattice (H_1 or H_2). This internal structuring is the basis for the attempts to use copolymer microemulsions as templates for designed nanostructured polymers or inorganic materials.[10,11]

Only a few studies have dealt with the temperature-dependent properties of microemulsions based on amphiphilic triblock-copolymers,[26,32−35] and almost nothing is known for the low-temperature side of the L_2-stability range. This is surprising since in many applications temperature is an important parameter. From studies of microemulsions with ordinary surfactants, temperature is known to have a great influence on the microemulsion properties and dynamics.[25,27,28] In light of this, the knowledge and understanding at present is still insufficient. Also unclear is the influence of the amphiphile polymeric nature as compared to the better investigated short-chained surfactants.

The present study, as part I of two publications, deals with the dynamic properties of microemulsions in the L_2-phase with $EO_{13}PO_{30}EO_{13}$ as stabilizer and *p*-xylene as oil. The varied system parameters are temperature and water content. We show that these parameters have indeed a strong influence on the microemulsion properties, however, in a different way than usually observed with microemulsions based on nonionic or ionic surfactants. A pronounced temperature-dependent tendency for reverse micelle to cluster and to form a transient network governs many physical properties of the triblock-copolymer microemulsions. We also elucidate the physical origin of the previously reported percolation transition,[33,35] and clarify the nature of large secondary aggregates previously reported as being lamellar.[26,36] Furthermore, we solve an apparent inconsistency in the literature: Addition of PEO−PI−PEO to w/o-microemulsions leads to significant droplet interconnection, which is reflected in a strong viscosity increase,[37,38] but a high microemulsion viscosity has not yet been established clearly for L_2-systems with triblock-copolymer as only amphiphile.[29,33,36,39,40] In the forthcoming study, part II, the reverse micelle properties will be examined as a function of temperature and water content.

Experimental Section

Chemicals. *p*-Xylene (purity > 99%) was purchased from Merck. The triblock-copolymer $EO_{13}PO_{30}EO_{13}$ (Pluronic L64 with nominal molecular mass 2900 g mol^{-1}, batch nos. WPDR-567-B and WPCR 5760) was kindly provided by the BASF Co., Mount Olive, NJ. Water cleaned by a Milli-Q purification system was used for the aqueous subphase in the microemulsions, with KCl (Merck, p.a. grade) added to yield 0.1 mol dm^{-3}. The probe $Ru(bpy)_3Cl_2$ (tris(2,2′-bipyridine)ruthenium(II)chloride) and the quencher methyl viologen (MV, 1,1′-dimethyl-4,4′-bipyridinium dichloride) were obtained from Sigma and were used as supplied. $Tb(pda)_3^{3-}$ (pda = pyridine-2,6-dicarboxylic acid) was prepared according to the method of Barela and Sherry.[41] Terbium chloride (Fluka, 98%) and ligand, pyridine-2,6-dicarboxylic acid (Merck, z.S.), were dissolved in a 0.02 mol dm^{-3} buffer solution of tris(hydroxy-methyl)-aminomethane (Merck, p.a.) also containing 0.1 mol dm^{-3} KCl. The $TbCl_3$ concentration was 0.1×10^{-3} mol dm^{-3} in a 2.3-fold excess of ligand (1×10^{-3} mol dm^{-3}). To increase the anionic ligand concentration, the pH of the buffer solution was adjusted to 8 with concentrated HCl (Merck, p.a.).

Microemulsions. The microemulsions were prepared from a mixture of *p*-xylene with Pluronic L64 at $m_p' = 0.4$, the triblock-copolymer mass fraction in oil. Aqueous solutions were added to the required mass fractions $m_w = 0.08$, 0.10, and 0.12 in the final mixture, respectively. The corresponding *z*-values (=[H_2O]/[EO]) were 1.35, 1.72, and 2.11. Manual shaking of the mixture at "room-temperature" resulted in all cases in optically transparent single-phase microemulsions. The temperature in the experiments was controlled with an accuracy of better than ±0.2 °C. No phase transition was observed in the entire investigated temperature range from 11 to 50 °C. The total quencher concentration in microemulsions C_q was calculated with

$$C_q = C_q^* \gamma_w \frac{\rho_m}{\rho_w} \quad (1)$$

were C_q^* is the quencher concentration in the aqueous solution, γ_w is the mass fraction of water in the microemulsion, ρ_m is the microemulsion density (0.93 at 22 °C and $m_w = 0.12$), and ρ_w is the water density.

Static Methods. The electric conductivity was recorded with a WTW LTA-1 electrode connected to a Tinsley Prism Instruments LCR Databridge 6458 with capacity compensation. The operating frequency was 1 kHz. Rheology was measured with a Bohlin Visco 88 Rheometer (Couette geometry with concentric cylinders). For the solvent *p*-xylene and triblock-copolymer solutions therein an Ubbelohde capillary viscometer (calibrated with distilled water) was used.

Luminescence Quenching. The $Ru(bpy)_3^{2+}$ concentration in the aqueous phase was 0.4×10^{-3} mol dm^{-3}, and the quencher concentration was varied between 1 and 4×10^{-3} mol dm^{-3}. Luminescence decays on the nanosecond time scale were measured with a single-photon counting setup. The frequency-doubled, ps-pulsed emission of a mode-locked Nd:YAG-laser (Spectra Physics model 3800) synchronously pumped a cavity-dumped dye laser (Spectra Physics model 3500) filled with the dye DCM. The dye-laser emission at $\lambda = 640$ nm and pulse repetition frequency 80 kHz was frequency doubled to give excitation pulses at the wavelength $\lambda = 320$ nm with a pulse width of <0.5 ns. The emission from the samples in 1 cm^2 quartz cells was registered by a Hamamatsu microchannel plate photomultiplier R1645U after passing through a 600 nm band-pass filter. The electronic signal processing consisted of an HP 8447F amplifier, a Tennelec TC 454 pulse discriminator, a Tennelec TC 861A time-to-amplitude converter, a Nuclear Data ND 579 AD-converter with 512 channels, and a microcomputer. Data accumulation was performed to obtain at least 10^4 counts collected in the peak-channel. A nonlinear least-squares procedure was used for data fitting.

$Tb(pda)_3^{3-}$ decays were recorded with a Perkin−Elmer LS 50 B spectrometer. The probe concentration was 0.1×10^{-3} mol dm^{-3}. The original cell holder for 1 cm^2 quartz cuvettes was rebuilt to attain a better temperature control. The excitation light source was a xenon flash-lamp (50 Hz) with 20 kW pulse power and 10 μs half-peak width. For excitation $\lambda = 320$ nm was selected, and phosphorescence emission was detected at $\lambda = 492$ nm. The registration unit was an EMI 9781B photomultiplier in analogue mode. The gate time was 10 μs and the integration time was 9.98 s. The time-resolved intensities were averaged from 499 pulses for each data point. Linear fittings were calculated on a microcomputer with a least-squares-fit method.

Dynamic Light Scattering. All samples were filtered through Sartorius Minisart filters with cellulose acetate membranes of 0.2 or 0.45 μm pore diameter. The continuous, vertically polarized emission of a frequency-stabilized Ar^+-laser at $\lambda = 488$ nm (Coherent Innova 300) in the light-mode was used to record the intensity autocorrelation function. The scattered light was registered behind a focusing lens and a 4 μm diameter

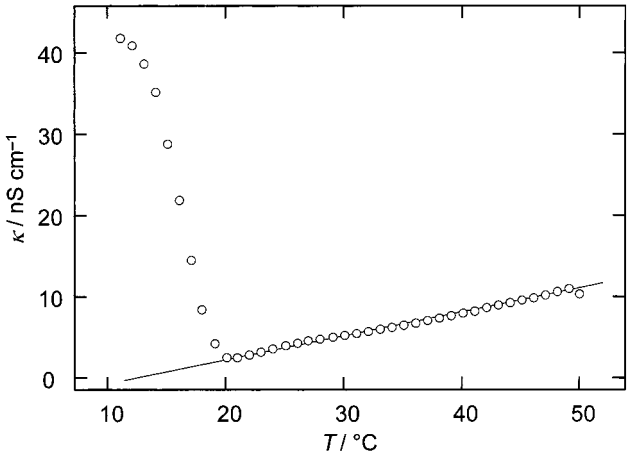

Figure 1. Electric conductivity κ of the microemulsion with *p*-xylene, $PEO_{13}PPO_{30}PEO_{13}$ and salt solution (0.1 mol dm^{-3} KCl) at $m_p' = 0.4$ and $m_w = 0.12$, as function of the temperature.

monomodal fiber (OZ Optics Montreal) by an ITT FW 130 photomultiplier operated in single-photon counting mode. The autocorrelator was an ALV 5000 wide-band digital autocorrelator installed in a microcomputer. The autocorrelation functions $g_2(t)$ were analyzed with the program package GENDIST.[42] An inverse Laplace transformation assuming a sum of Gaussian peaks was performed to obtain the relaxation time distribution function $\tau A(\tau)$ versus log τ by using the constrained regularization program REPES.[43] The range of relaxation times allowed fitting between 10 μs and 100 s with the point density 12 per decade. The apparent diffusion coefficients D are related to the relaxation rate Γ and the scattering vector $q = 4\pi n\lambda^{-1} \sin(\theta/2)$ by $D_{app} = \Gamma q^{-2}$, where $n = 1.4672$ is the refractive index (measured with an Abbé-refractometer using polychromatic light) of the microemulsion at $m_w = 0.12$, 1.4705 at $m_w = 0.10$, and 1.4735 at $m_w = 0.08$, and θ is the angle between primary and scattered beams.

Results and Discussion

Electric Conductivity. The electric conductivity κ of the microemulsion with $m_p' = 0.4$ and $m_w = 0.12$ is shown in Figure 1. In the temperature range between 45 and 20 °C, κ is small and decreases monotonically upon temperature decrease. Here the microemulsion behaves as a dispersion of conducting particles (the reverse micelles containing the salt solution) in the nonconducting organic solvent. The trend of κ in the poorly conducting region can be understood from an increased solvent viscosity and reduced charge fluctuations at lower temperature, following a model suggested by Eicke et al.[44] However, a sudden and characteristic increase of κ occurs from a temperature just below 20 °C until the phase boundary is reached close to 11 °C (the melting temperature of pure *p*-xylene is 13.2 °C). This shows that an additional pathway for charge-carrier migration takes over. The microemulsion was isotropic at all temperatures, but it exhibits flow birefringence at $T < 23$ °C upon stirring. It is noteworthy that the microemulsions with lower water content, $m_w = 0.10$ and 0.08, do not show a similar κ-increase.

Such transitions from a low to a high conducting state are frequently observed in oil-rich microemulsions based on short-chained nonionic surfactants of the C_iE_j-type and are discussed as percolation transitions.[25,45−47] Such transitions also occur in microemulsions with ionic-surfactants, although, with the opposite temperature dependence.[28,46,48,49] Two different mechanisms of structural evolution have been suggested to explain this phenomenon. The first, equivalent to the static percolation model,[50] assumes a transformation of the microemulsion containing dispersed droplets into a bicontinuous system.[25,27] The origin is considered to be enhanced hydration of the polar surfactant moieties at lower temperature, which leads to a change in the mean monolayer curvature from negative (as defined for the monolayer curves toward water) to almost zero or positive values.[25,27,52] This model is frequently discussed for microemulsions with nonionic surfactants. However, also an alternative theory is frequently discussed in the literature. This second model, corresponding to dynamic percolation,[50] explains the observed phenomenon by an aggregation of droplets into extended clusters, which is accompanied by a rapid exchange between the individual compartments. The clustering model is mostly used for microemulsions with ionic surfactants. Entropy gain has been suggested as the driving force for the secondary aggregation,[28,48] possibly a consequence of released solvent molecules from a confined state in the monolayer into the bulk.[28,53] From the observed temperature dependence it can be concluded that microemulsions with amphiphilic triblock-copolymers behave similarly to those with nonionic surfactants. In the next sections we will elucidate details of the percolation-like transition by means of dynamic methods and clarify its physical origin.

Time-Resolved Luminescence Quenching. First measurements on the sub-microsecond time-scale using the probe $Ru(bpy)_3^{2+}$ in combination with the quencher MV^{2+} are discussed. Due to the ionic character of both probe and quencher, these molecules are usually assumed to be exclusively solubilized in the cores of reverse micelles (where also the water is localized). Two sets of typical decay curves with varied quencher concentration in the microemulsion at $m_p' = 0.4$ and $m_w = 0.12$ are shown in Figure 2. The upper diagram corresponds to $T = 40$ °C, the lower to $T = 16.5$ °C. Two different states belong to these depicted decay sets as it can been inferred from comparison with Figure 1. In the logarithmic representation of the intensity as a function of time a nonexponential decay occurs at the beginning. This shows the compartmentalized internal structure of the microemulsion with amphiphilic triblock-copolymer, where the fast process stems from energy transfer between excited probe and quencher confined within the same reverse micelle.[55] At longer times, after about 300 ns, the curves evolve single-exponentially. The almost parallel tails at high temperature indicate a slow exchange of probe and quencher between the reverse micelles, whereas at low temperature this has changed implying an accelerated exchange. As it is usually found in luminescence quenching studies with short-chained surfactants forming spherical aggregates, the decays could be well described by the Infelta−Tachiya equation:[56,57]

$$I(t) = I_0 \exp(-A_2 t - A_3(1 - \exp(-A_4 t))) \qquad (2)$$

This statement also holds for the other investigated temperatures and water contents. The decay profiles, the systematic trend of the reverse micelle radius with T (subject in part II of this series) and the fact that no temporal extension of the intramicellar quenching reaction could be observed when T is lowered provide a strong argument for a maintenance of the globular aggregate shape in the entire investigated temperature range, including the state of high electric conductivity. No indication for an aggregate growth toward elongated rods could be detected, as it was for example observed with C_iE_j w/o-microemulsions at high water amount and low temperature.[58]

Under the conditions that (a) both the probe and quencher are confined exclusively to the minority water phase of the microemulsion, (b) they are independently distributed over the

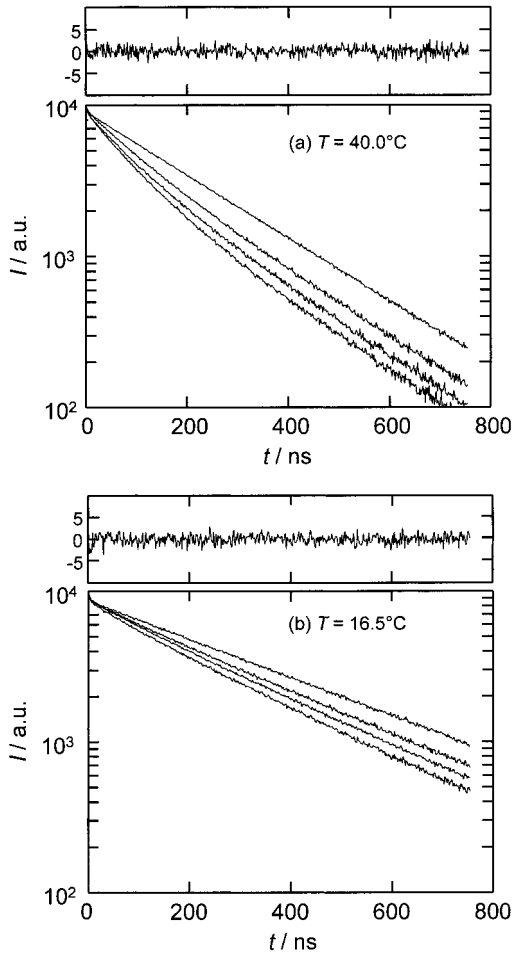

Figure 2. Time-resolved luminescence decay curves at $T = 40$ °C (a) and 16.5 (b) for the microemulsion $m_p' = 0.4$, $m_w = 0.12$ with different quencher concentration in the aqueous phase (C_q* between 0 and 4 × 10^{-3} mol dm^{-3}). The top curves correspond to quencher-free microemulsion, respectively. The weighted residuals shown correspond to fits using eq 2 to the decays with $C_q^* = 4 \times 10^{-3}$ mol dm^{-3}. The probe was $Ru(bpy)_3^{2+}$, quencher was MV^{2+}. In all cases the reverse micelle concentration $C_m < 1.1 \times 10^{-3}$ mol dm^{-3} and the average quencher number per reverse micelle was < 0.5.

compartments obeying the Poisson-distribution, and (c) any exchange only takes place on direct droplet contact with subsequent fusion, then the experimental parameters A_2-A_4 in eq 2 for microemulsions are given by:

$$A_2 = k_0 + \frac{k_{ex}k_{qm}}{k_{qm} + k_{ex}C_m}C_q \qquad (3)$$

$$A_3 = \left(\frac{k_{qm}}{k_{qm} + k_{ex}C_m}\right)^2 \frac{C_q}{C_m}$$

$$A_4 = k_{qm} + k_{ex}C_m$$

as it was shown by Atik and Thomas.[59] Here $k_0 = 1/\tau_0$ is the rate of natural luminescence deactivation and C_q is the quencher concentration. These expressions allow the determination of the micelle concentration C_m, the rate constant of intradroplet quenching k_{qm}, and the exchange rate constant k_{ex}. The former two quantities will be dealt with in a forthcoming study on the aggregate properties with amphiphilic triblock-copolymer.

Since it was established recently that two principally different exchange mechanisms may play a role for exchange between the compartments,[28,54] also the luminescence quenching behavior

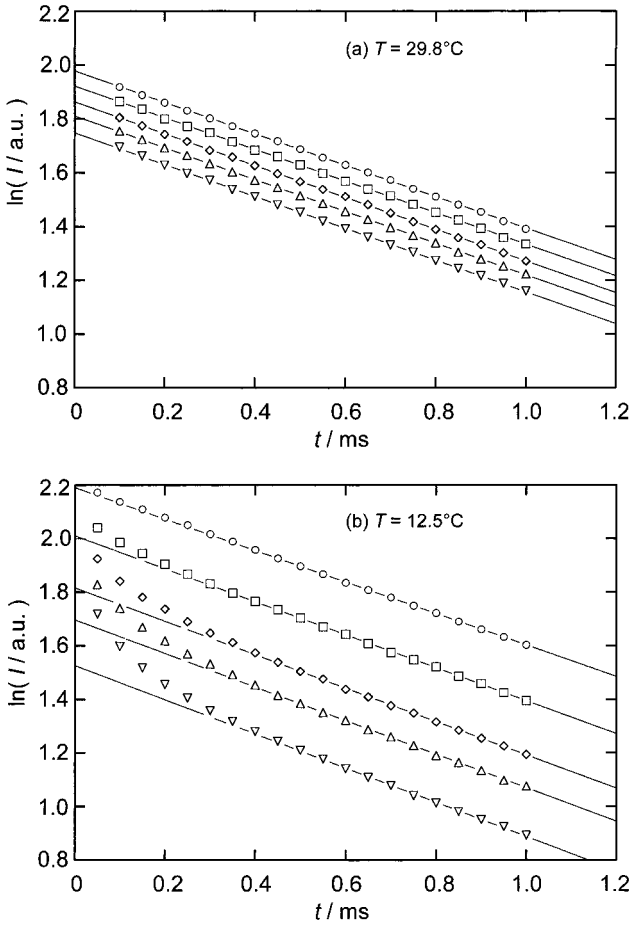

Figure 3. Time-resolved luminescence decay curves for the same microemulsion as in Figure 2 but using the probe $Tb(pda)_3^{3-}$. Note the long experimental time scale. $T = 29.8$ °C (a) and 12.5 °C (b). The top curves correspond to the quencher-free microemulsion, and C_q* ranges between 31 × 10^{-6} and 124 × 10^{-6} mol dm^{-3}. Quencher was MV^{2+}.

on the millisecond time scale was studied using the probe $Tb(pda)_3^{3-}$ ($\tau_0 = 2$ ms) in combination with MV^{2+}. These mechanisms, occurring well separated in time, exchange within clusters and exchange between free droplets or clusters. The clusters can be formed from several droplets associated in a secondary aggregate. In particular, reverse micelles based on triblock-copolymers are suspected to be effectively linked, since two hydrophilic moieties are present in the same amphiphile molecule. Figure 3 shows decays on the millisecond time scale obtained for the microemulsion at $m_w = 0.12$ and two temperatures (29.8 and 12.5 °C). The decay profiles are found to be completely different from those obtained on the shorter time scale: The final exponential tails are almost parallel at both the high and low temperature, and with the same slope as in quencher-free solutions. At 12.5 °C, however, an additional, nonexponential process shows up, which decays at about 0.4 ms. This quenching reaction was observed to evolve gradually between 29.8 and 15 °C, but it does not gain more importance below 15 °C. This finding provides evidence for clusters governing the decay behavior in the microemulsion. The rapid exchange occurring on the sub-microsecond time scale (detected by using $Ru(bpy)_3^{2+}$ and characterized by k_{ex},) is thus an exchange within a cluster. This is accelerated (as we will discuss in detail below) by a temperature-related, gradual cluster growth, which stands in contrast to the sudden increase of the electric conductivity.

Different approximations for quenching reactions within clusters have been proposed by Almgren and Johannsson.[54] As it can be inferred from the dependence of the decay constant on the quencher concentration, the clusters are not fully explored on the sub-microsecond time scale. This corresponds to the situation of large clusters and low quencher concentrations as discussed in ref 54. The approximate decay-function within the random-walk model reads

$$\ln\frac{I(t)}{I_0} = -k_0 t - nS(k_w t) \tag{4}$$

where $n = C_q/C_m$ is the average occupation number of micelle with quencher, and $S(k_w t)$ is the number of visited sites (micelles) by the random walk with step frequency k_w. For a compact cluster geometry $S(k_w t)$ is given by

$$S(k_w t) = a_2(k_w t) \tag{5}$$

and for fractal aggregates is

$$S(k_w t) = a_2(k_w t)^{d_s/2} \tag{6}$$

where a_i are constants and d_s is the spectral dimension of the cluster. If the clusters were loose and highly ramified, a deviation from an exponential decay behavior is expected according to eq 6, which was not observed in experiment. The clusters appear thus as compact entities, which is not surprising for the present high volume fraction of reverse micelles. For an application of eq 4 it needs to be extended in order to account for intramicellar quenching and exchange between clusters. Since the decay within a compact cluster occurs single-exponentially, eqs 2−4 can be combined, leading to

$$k_{ex} = \frac{a_1 k_w}{C_m} \tag{7}$$

when $k_{qm} \gg k_{ex}C_m$. The second-order rate constant k_{ex} now characterizes the exchange within a cluster. On the other hand, for measurements on the long time scale when the energy transfer within clusters has decayed, the slow exchange becomes apparent and the decay law is

$$\ln\frac{I(t)}{I_0} = k_0 t - n_c - k_{cc}C_q \tag{8}$$

where n_c (apparent initial drop) is given by the average cluster occupation number with quencher, and k_{cc} is the second-order rate constant for the intercluster exchange.[28] Although it is difficult to evaluate the initial drop quantitatively (due to a contribution coming from analogue detection), n_c in Figure 3 at constant C_q increases when lowering T. This is a direct consequence of a decreasing cluster concentration C_c (since $n_c = C_q/C_c$) due to cluster growth. The intercluster exchange is fastest at 11 °C with $k_{cc} \leq 4 \times 10^6$ s^{-1} mol^{-1} dm^3, which is at least 500 times less than k_{ex}. The rate constants k_{cc} at higher temperature are too small to be determined precisely in the tolerable quencher concentration range, even with the long probe lifetime $\tau_0 = 2$ ms. It is interesting to note that the first-order decay constant 1.1×10^4 s^{-1} of the fast process in Figure 3 (estimated for 12.5 °C and highest quencher concentration) divided by $C_q = 1.38 \times 10^{-5}$ mol dm^{-3} results in a second-order rate constant 8×10^8 s^{-1} mol^{-1} dm^3, which is of the same order of magnitude as k_{ex} obtained from the sub-microsecond time scale (see Table 1 and Figure 4).

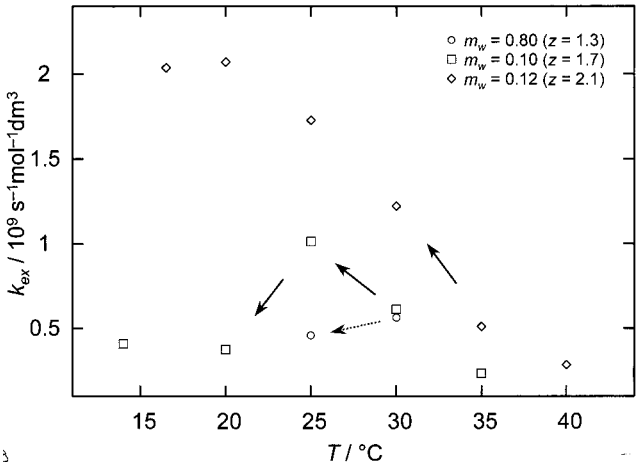

Figure 4. Intracluster exchange rate constant k_{ex} in $EO_{13}PO_{30}EO_{13}$ w/o-microemulsions as function of temperature and water content m_w (z = [H_2O]/[EO]).

TABLE 1: Values of Fast (k_{ex}) and Slow (k_{cc}) Exchange Rate Constants for Various Microemulsion Conditions

	$k_{ex}/10^9$ s^{-1} M^{-1}			$k_{cc}/10^6$ s^{-1} M^{-1}
T/°C	$m_w = 0.08$	$m_w = 0.10$	$m_w = 0.12$	$m_w = 0.12$
11.0				≈4.0
14.0		0.41		
16.5			2.04	
20.0		0.20	2.07	
25.0	0.46	1.01	1.73	
30.0	0.57	0.61	1.22	
35.0		0.24	0.51	
40.0			0.29	

For an understanding of the percolation-like transition a consideration of the dependence of k_{ex} on temperature and water content is straightforward, since the transport of charge carriers through the microemulsion is closely related to the exchange rate. The expressions in eq 3 were derived from a theory considering only quencher exchange, while in the present case both the probes and quenchers can undergo exchange, leading to a larger k_{ex}. However, Lang et al. have discussed the corresponding deviations to be less than 20%,[48] therefore we use eq 3 for simplicity. With the microemulsion showing percolation, $m_w = 0.12$, k_{ex} increases considerably upon lowering the temperature as it can been seen from Figure 4 and Table 1. Already on the high-temperature side k_{ex} is accelerated, however, it reaches a maximum where also κ starts to diverge. This implies that the cluster growth at $T = 20$ °C has advanced to the first "infinite" aggregate, and a further aggregate linkage affects only the electric conductivity. The exchange rates for $m_w = 0.10$ and 0.08 are generally smaller, and also their trend with T inverts via $m_w = 0.10$ to $m_w = 0.08$. For $m_w = 0.10$ there is a distinct maximum of k_{ex} at 25 °C, while for $m_w = 0.08$ even an deceleration of quenching is observed when lowering T. This observation can be explained by water binding to the hydrophilic ethylene oxide moieties. For $m_w = 0.12$ the microemulsion contains $z = 2.11$ water molecules per EO unit, $z = 1.72$ for $m_w = 0.10$, and only $z = 1.35$ for $m_w = 0.08$. When the water content is small, the competition for hydration water between ionic solutes and the polar headgroups is expected to be stronger, leading to a reduced ion mobility. One effect of reducing the temperature is that water binding to ethylene oxide (and propylene oxide) moieties gains importance,[7] Hence, this also may suppress an high ion mobility. This effect does not play the dominating role at the highest water content, but at $m_w = 0.10$ and below $T = 25$ °C it is already counteracting the ion

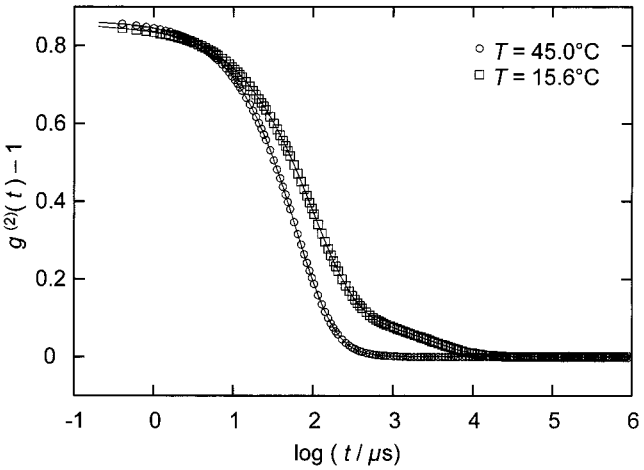

Figure 5. Examples of intensity autocorrelation functions measured with amphiphilic triblock-copolymer w/o-microemulsion at $m_w = 0.12$. The fits belong to inverse Laplace transformation. For characterization of the microemulsion state cf. Figure 1.

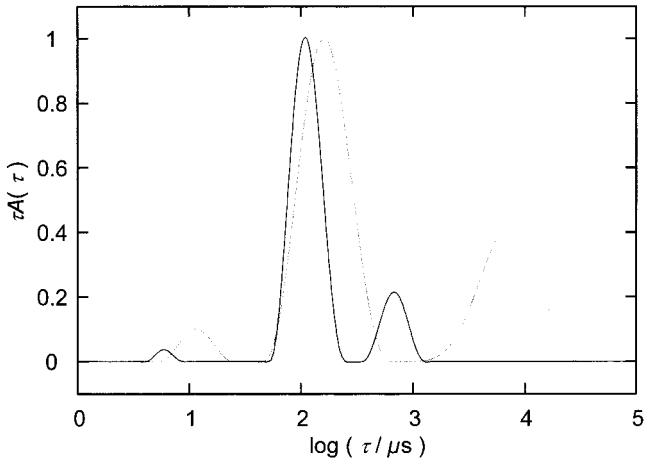

Figure 6. Relaxation time distribution as obtained by inverse Laplace transformation. These trimodal distributions correspond to the correlation functions in Figure 5. The black curve is for $T = 45.0$ °C and the gray for $T = 15.6$ °C.

migration within clusters and becomes even more important (i.e., the effect is shifted to higher temperature) for $m_w = 0.08$. Through the consideration of k_{ex} it becomes obvious why the percolation-like transition did not occur for microemulsions with $m_w < 0.12$.

The exchange between clusters may be expected to be diffusion controlled when the system is percolated, i.e., the encounter of a cluster with excited probe with one containing quencher leads to probe deactivation. The diffusion-controlled rate constant k_{dc} for reactions in *p*-xylene at 20 °C is calculated to be 1.05×10^{10} s^{-1} dm^3 mol^{-1}, using the relation $k_{dc} = 8RT/3\eta_0$ for spheres and $\eta_0 = 0.6185$ Pa s.[60] From comparison with the experimental data it turns out that k_{cc} is at least by the factor 2600 slower. It is hard to believe that only energetic demands due to an ion immobilization are responsible for this great reduction. It appears more reasonable that mixing of the aqueous micelle interior is strongly hindered through steric constraints, which arise from the polymeric nature of the amphiphile. Also, a stiffening of the hydrated ethylene oxide chains in the reverse micelle core at lower temperature may influence the very slow intercluster exchange.

It is interesting to compare the results from luminescence quenching to water diffusion in L_2-microemulsions with $EO_{13}PO_{30}EO_{13}$. In a recent study it was reported that the self-diffusion coefficient of water at 25 °C is much faster ($\approx 10^{-10}$ m^2 s^{-1}) than that of triblock-copolymer (5×10^{-14} m^2 s^{-1}),[40] although for an oil-continuous droplet structure these self-diffusion coefficients are expected to be almost equal. Combining the findings leads to the conclusion that an additional pathway for water migration (but not for ions) exists. Since also PPO may bind water at lower temperature,[61] it is a reasonable picture that water migration along the polymer backbone, including the "hydrophobic" amphiphile middle-block, occurs. Unfortunately, such a transport mechanism cannot be probed by the TRLQ-technique and other appropriate methods have to be applied to prove this hypothesis.

Dynamic Light Scattering. The presented picture of the structural evolution is corroborated by results from the dynamic light scattering experiments. The time-averaged intensity was found to be constant in the temperature range from 35 down to 11 °C, confirming the conclusion from luminescence quenching that no temperature-induced growth of the reverse micelle toward elongated micelles occurs. Figure 5 shows autocorrelation functions measured for $m_w = 0.12$ at two different states of conductivity. Clearly, a slow relaxation mode can bee seen at $T = 15.6$ °C. Analyzing these intensity autocorrelation functions by inverse Laplace-transformation, three well-separated modes appear in both relaxation time distribution function as shown in Figure 6.

The average relaxation rates Γ ($=1/\tau$) corresponding to the peak maxima are proportional to q^2, respectively. This demonstrates the diffusive nature of all three processes. The apparent diffusion coefficient D_1 of the fast mode is between 0.7×10^{-10} (12.1 °C) and 2.4×10^{-10} m^2 s^{-1} (45.0 °C) and is attributed to the translational diffusion of molecularly dissolved polymer, so-called unimer. The second and dominant mode with $D_2 \approx 10^{-11}$ m^2 s^{-1} reflects the mutual diffusion of reverse micelles. At $T = 25.0$ °C is $D_1 = 1.5 \times 10^{-10}$ m^2 s^{-1}, which is a factor 3 larger than the self-diffusion coefficient of $EO_{13}PO_{30}EO_{13}$ in pure *p*-xylene ($D = 5 \times 10^{-11}$ m^2 s^{-1} from linear extrapolation in Figure 5 in ref 40 to $\phi = 0.435$). This difference is probably an effect of rapid thermodynamic particle fluctuations, despite the present attractions.[62] An interesting aspect is that attempts to investigate the molecular dissolved triblock-copolymer in solution by light scattering failed, since the refractive index difference between *p*-xylene and $EO_{13}PO_{30}EO_{13}$ is too small. The fact that the autocorrelation functions from measurements with the ternary mixtures contain a contribution of the unimer implies that some water molecules are bound to the nonaggregated triblock-copolymer. This also accounts for the relative intensity of the unimer peak becoming greater at lower temperature (gray line in Figure 6), although the so-called critical microemulsion concentration ($c\mu c$) is then smaller.[14]

Neither D_1 nor D_2 varied significantly upon changing m_w. However, temperature has a strong influence on the cooperative diffusion coefficients, where D for both involved species decreases strongly when lowering T. It was shown recently that renormalization of D_1 with respect to temperature and viscosity according to the Stokes−Einstein relationship

$$r_h = \frac{k_B T}{6\pi\eta_0 D} \tag{9}$$

does not result in constant values proportional to the hydrodynamic radius r_h, still $D_1\eta_0/T$ was a linear function of T.[35] This was interpreted as a consequence of attractive interactions among the polymer molecules governing the diffusive behavior, which increase when lowering T.[35]

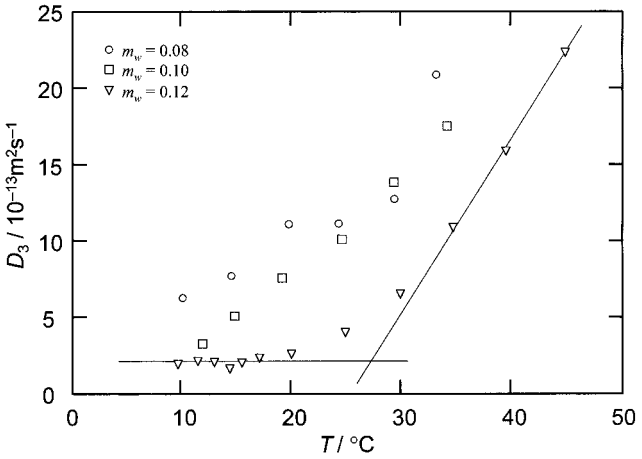

Figure 7. Apparent cluster diffusion coefficient D_3 as function of temperature.

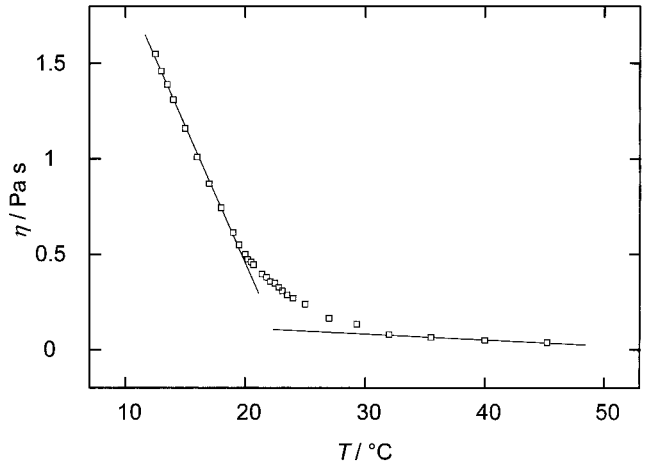

Figure 8. Low-shear viscosity of L_2-microemulsion, $m_w = 0.12$, with $EO_{13}PO_{30}EO_{13}$ measured at $\dot{\gamma} = 24.2$ s^{-1}.

The slowest component has D_3 in the range of 2×10^{-13} to 2.2×10^{-12} m^2 s^{-1} and is attributed to the diffusive motion of larger aggregates, the clusters. An important result is that the third diffusive process is present in the whole temperature range, implying that clusters already exist far from the percolated state at high temperatures. This is a consequence of the general linking capability of the triblock-copolymer. The relative importance and width of the slow relaxation mode increases at lower temperature (cf. Figure 6). It is interesting to note that a percolated microemulsion with ionic AOT as surfactant, where extended but highly dynamic clusters are assumed to be present, does not show any slow relaxation mode in the autocorrelation function.[63] D_3 has the most pronounced temperature dependence. Considering the microemulsion at $m_w = 0.12$, D_3 in Figure 7 first decreases linearly when T is lowered, in contrast to the abrupt κ-change but in agreement with the gradual increase of k_{ex}. D_3 starts to level out at 25 °C, and reaches constant values at 20 °C. Here, where the clustering has evolved to an "infinite" network at the percolation threshold, the mobility of the network becomes slower than the diffusive motion of a time-averaged cluster.

Inherent to the effect of particle interactions in concentrated systems is the complication, that true hydrodynamic radii according to eq 9 cannot be obtained.[62] One way to estimate the magnitude of interactions changing r_h is to compare the apparent hydrodynamic reverse micelle radius $r_{h,app}$ with r_h determined by other, less-interaction-sensitive methods. Such radii could reasonably well be estimated from self-diffusion measurements with pulse-gradient spin−echo NMR.[40] The value for r_h corresponding to the system of interest here ($m_w = 0.12$) is 11.5 nm at $T = 25.0$ °C, from which the correction factor $c = 0.347$ is deduced. When it is assumed that the reverse micelles and the large aggregates are influenced by the interactions in the same way and strength, and that the cluster behaves hydrodynamically as a sphere, one obtains with $D_3 = 4.0 \times 10^{-13}$ m^2 s^{-1} and $\eta_0 = 0.5948 \times 10^{-3}$ Pa s at $T = 25.0$ °C (cf. next section) $r_h = c\, r_{h,app} \approx 320$ nm. This would correspond to about 2×10^4 single spheres in dense packing, but less in random packing. In view of the evolution of the microemulsion structure toward an infinite network at 20 °C, this estimation seems to be reasonable.

For systems containing less water the cluster mode is present as well, in the entire temperature range. However, at a given temperature D_3 is the larger the smaller the water content. Furthermore, a plateau at the low-temperature side is not reached for $m_w = 0.10$ and 0.08. The finding of water favored cluster growth, also previously noticed by Chu et al. from the relative importance of the slow relaxation mode,[26,36] explains the observation of an strong reduction of the triblock-copolymer self-diffusion coefficient with m_w (or z), which far exceeds obstruction effects.[40] The network built-up and properties, mainly influenced by the temperature-dependent solubility of the ethylene oxide chains in *p*-xylene and the configuration of the propylene oxide moieties, are in a first consideration not expected to vary much with the small changes in water content. That there is a dependence though, indicates that the water in the reverse micelles acts as "glue" for ethylene oxide. The better the poly(ethylene oxide) hydration is (with more water) the more difficult it is for the PEO moieties to escape into the continuous phase. As consequence, the linkage lifetime increases with the water content, leading to larger time-averaged aggregates. However, this idea is in contradiction to recently reported triblock-copolymer lifetimes in a reverse micelle, where a lifetime decrease was discussed to occur with increasing water content.[34] This question still needs to be clarified.

Chu and co-workers have reported similar large aggregates coexisting with micelles and unimers, and describe their amount and size to obey the same temperature trend as in the present study.[26,36] However, they suggest the internal structure of the large aggregates to be lamellar and present their image graphically in ref 36. The results in the present study, in particular considering luminescence quenching but also the constant scattering intensity and occurrence of clusters at high temperatures, let one exclude such a structure to be responsible for the observed phenomena.

Viscosity Measurements. For a further characterization of the temperature-induced structural changes, rheological measurements were performed. The apparent viscosity shown in Figure 8 for $m_w = 0.12$ was measured at low shear rate, $\dot{\gamma} = 24.2$ s^{-1}. This shows principally a similar pattern as the conductivity curve, but with the important difference that the divergence starts already at 30 °C. From that it is again obvious that the structural evolution occurs considerably earlier than the onset of percolation. Exactly the same course is observed for the relative viscosity $\eta_r = \eta/\eta_0$, since η is exceeding η_0 by far. With *p*-xylene, η_0 was measured to be 0.5154×10^{-3} Pa s at $T = 40$ °C, increasing to 0.5948×10^{-3} Pa s at $T = 25.0$ °C. This results in $\eta_r = 97$ at 40 °C and 402 at 25 °C, and the maximum value is 2500 at 12.5 °C. These relative viscosities are extraordinarily high. To provide values for a comparison, Eshuis and Mellema found η_r for a nonionic L_1-microemulsion to remain below 3.5 at the dispersed phase volume fraction ϕ

≈ 0.24,[64] Smeets et al. found with the L_2-phase of AOT a η_r -range between ≈ 1 and 18 with $0.03 < \phi < 0.4$,[65] and for a percolating nonionic w/o-microemulsion Schlicht et al. reported $\eta \approx 16 \times 10^{-3}$ Pa s, which corresponds to $\eta_r \approx 25$.[66]

For describing η_r of a hard-sphere dispersion taking interparticle effects at higher volume fractions into account, the semiempirical Simha expression may be used:[67]

$$\eta_r = 1 + \frac{10\phi R^3(R^7 - 1)}{4(R^{10} + 1) - 25(R^7 + R^3) + 42R^5} \quad (10)$$

where R is given by

$$R = f\phi^{-1/3} \quad (11)$$

In this formulation f is a parameter depending on particle shape and interactions, which is one or slightly above for hard spheres.[64] Taking $\phi = 0.435$ (calculated from all the copolymer and water in the microemulsion) results in $f = 0.864$, 0.820, and 0.790 for $T = 40$, 25, and 12.5 °C, respectively. That the parameter deviates considerably from unity is again a reflection of the strong attractive aggregate interaction. A characteristic of w/o-microemulsions with amphiphilic triblock-copolymer is the high molecular solubility of the amphiphile in oil, i.e., material which is not incorporated in the reverse micelles (unimer). From water solubility studies the *cμc* was found to be about 9% triblock-copolymer at 25 °C and 14% at 40 °C.[14] Since this may change the microemulsion properties to a large extent, also η_r' based on the viscosity of a molecular copolymer solution is considered. The latter viscosities were 1.279×10^{-3} Pa s at $T = 40$ °C and 0.951×10^{-3} Pa s at $T = 25$ °C, resulting in $\eta_r' = 39$ at 40 °C and 251 at 25 °C. The corresponding volume fractions obtained from subtracting the unimer amount are $\phi = 0.29$ (40 °C) and 0.36 (25 °C). The parameter f is then almost constant (0.775 and 0.776), implying an even stronger deviation from hard-sphere behavior in this consideration.

In their work on the viscosity of aggregating microemulsion droplets, Smeets at al. combine a virial expansion of η_r

$$\eta_r = 1 + \frac{5}{2}f\phi + \frac{5}{2}(1 + a_2)f^2\phi^2 + \ldots \quad (12)$$

with a temperature-dependent parameter $a_2(T)$, which contains the Gibbs free energy ΔG for clustering per mole contact points.[65] They derive for the second virial coefficient of the viscosity the following relationship:

$$a_2(T) = a_{2,0} + a_{2,1}\exp\left(-\frac{\Delta G}{RT}\right) \quad (13)$$

where $a_{2,0}$ is a constant due to the temperature-independent hard-sphere contributions. The structure factor f was found to be 1.04 and the constant $a_{2,0} = 2.6$. Within this model, a subtraction of the constants from η_r and combination of eqs 12 and 13 leads to a van't Hoff-type relationship. When these values of f and $a_{2,0}$, are used for the spherical aggregates in this study, such a relationship is indeed found. The corresponding plot is shown in Figure 9, where in contrast to the finding of Smeets et al. two regions with a crossover at 30 °C can be distinguished. For both regimes ΔG is negative with -38 kJ mol^{-1} on the high- and -107 kJ mol^{-1} on the low-temperature side. The fact that ΔG is more negative at low T indicates an enthalpy-driven process while the clustering entropy is positive, a view which is supported by the other applied methods. Smeets et al. argue that in their investigated temperature range over 25 °C the enthalpic and entropic contributions are temperature independent.[65] However, the kink observed in Figure 9 indicates a change in the aggregation thermodynamics, either of ΔH or ΔS, or both. Since many processes in the microemulsion are involved when the temperature is altered, i.e., changes of droplet sizes, solvent quality, copolymer hydration and configuration, interaction strength, etc., we refrain here from further speculation.

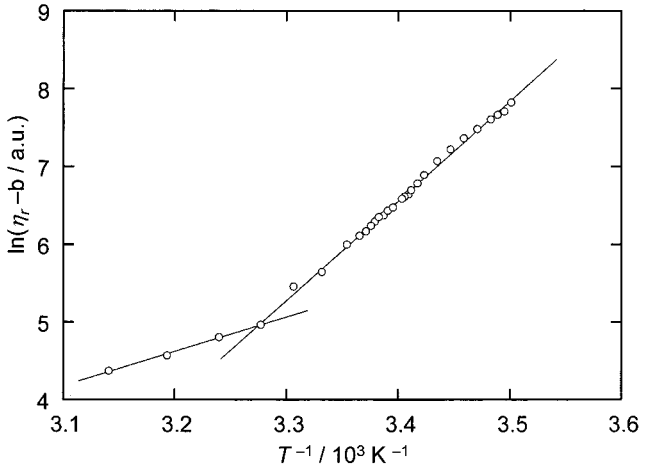

Figure 9. Van't-Hoff plot of the microemulsion relative viscosity η_r corrected by the constant $b = 1 + 2.5\ f\phi(1 + f\phi - a_{2,0}f\phi)$. For definitions see text.

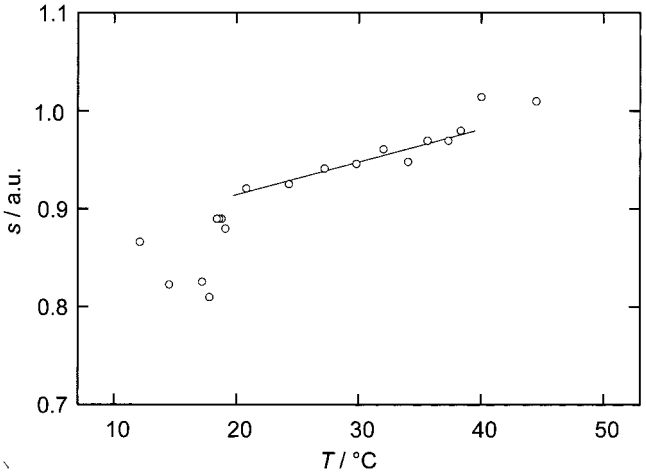

Figure 10. Pseudo-plasticity constant of the L_2-microemulsion at $m_w = 0.12$.

Additionally, the dependence of the apparent viscosity on the shear rate was investigated in the range between 24.2 and 1209 s^{-1}. A negative curvature was present in the plots of the shear stress σ versus $\dot{\gamma}$ at $T < 20.8$ °C, revealing a pseudo-plastic flow of the microemulsion. But no indications were found for a yield stress. These findings confirm the work of Wu and Chu, who also found no shear-rate dependence at (only measured) $T = 26.2$ °C.[36] In a log log-plot σ is a linear function of $\dot{\gamma}$, yielding from the slope the pseudo-plasticity constant s, which is shown in Figure 10. A simple Newtonian-flow is found at $T = 40$ °C and above, where s is close to unity. This constant then decreases linearly between 40 and 20.8 °C to 0.92, followed by a drop to about 0.8 over the narrow T range to 17.2 °C, in which also κ shows the increase. In the entire temperature range the microemulsion remained fluid, and no gel formation, as for example was observed from a cubic phase or with obstructing rodlike micelles in aqueous solutions of similar triblock-copolymers,[22,29] could be observed.

Oscillatory shear measurements show that there is no significant storage modulus for the triblock-copolymer micro-

emulsion. On the other hand, in a study on the associative behavior of semidiluted solutions of ionically end-capped polyisoprene in organic solvent, Johannsson et al. report an occurrence of high storage moduli attributed to a network.[21] The viscoelastic relaxation time ranged there between several tens of milliseconds to 100 ms and obeyed an Arrhenius-relationship yielding the activation energy of 25 kJ mol^{-1}, which was discussed as break-up energy of multiplets. Comparison shows that the network with triblock-copolymer must be much weaker with respect to external forces, implying smaller activation energies for link breakage and shorter characteristic connection lifetimes. This view is supported by the estimated equilibrium residence time of an amphiphilic triblock-copolymer molecule in a reverse micelle of the order of 10 ms.[34] The internal network structure can apparently instantaneously react on an applied shear. One response is that the clusters align in shear flow, explaining the observed flow birefringence. As revealed from static viscosity, however, aggregate rupture requires a higher shear force when T is low. This can be attributed to higher transfer energies for ethylene oxide moieties from the reverse micellar state into continuous *p*-xylene when the solvent quality becomes worse. Thus, the infinite network formed at the percolation threshold is weak and dynamic, but still stronger as in percolating ionic microemulsions as revealed from luminescence quenching and dynamic light scattering.

Amphiphilic Triblock-Copolymer versus Surfactant. The investigated L_2-microemulsions with amphiphilic triblock-copolymer show qualitatively some similarities to those with short-chained nonionic surfactants. These are mainly the occurrence of the electric percolation transition and the increase of viscosity upon lowering the temperature. Such observations have frequently been reported for microemulsions with C_iE_j or related surfactants.[25,45−47,66] However, the differences of surfactant systems to microemulsions with amphiphilic triblock-copolymer prevail as specified in the following.

The percolation phenomenon in typical surfactant L_2-microemulsions leads to a κ-increase over at least two decades, even at small salt concentration in the aqueous phase.[46] Here, using the amphiphilic triblock-copolymer, only an relative weak κ-increase (factor 16) is observed; the transition is much less pronounced. Also a comparison of the solute exchange rates shows remarkable differences. The solute exchange rate constant k_{ex} (measured with $Ru(bpy)_3^{2+}$) in microemulsions with C_iE_j reaches at the low-temperature side of one-phase stability 8×10^9 s^{-1} mol^{-1} dm^3, which close to the diffusion controlled limit.[68] Here, despite of the exchange mechanism, where k_{ex} remains below 2.1×10^9 s^{-1} mol^{-1} dm^3 considerably smaller values are found. The exchange rate k_{cc} on the millisecond time-scale, using $Tb(pda)_3^{3-}$, was found to increase from 1.6×10^8 to 3.2×10^8 s^{-1} mol^{-1} dm^3 for a nonionic L_2-microemulsion when percolated.[46] That system is comparable to the microemulsion $m_w = 0.12$ investigated here, since $W_0 = 12.2$ corresponds to $z = 2.44$ for the surfactant used. Here, however, k_{cc} was always $\leq 4 \times 10^6$ s^{-1} mol^{-1} dm^3. In contrast, although electric conductivity and exchange rates remain significantly smaller, the viscosity increase with the triblock-copolymer microemulsion is much stronger than that of percolating w/o-microemulsions with C_iE_j.[66]

The origin of electric percolation in nonionic microemulsions is believed to be a consequence of a structural transition from disconnected droplets to a dynamic bicontinuous structure, where the charge carrier can easily migrate within the aqueous channels temporarily formed.[25,27] Such a transition is excluded for systems with amphiphilic triblock-copolymer from the finding of clusters governing the solute transport properties. Different exchange mechanisms appearing on different time scales, as observed here, have not been established for nonionic microemulsions so far. Formally, this finding resembles more that of microemulsions with the ionic-surfactant AOT, where intra- and intercluster exchange processes have been identified.[28,54,55] But also with percolating AOT systems both the electric conductivity and exchange rates reach much higher values than found here. Furthermore, the temperature dependence of clustering is reverse, i.e., AOT w/o-microemulsion droplets aggregate with increasing temperature. This process has been discussed as entropy driven.[28] Here, from the found temperature dependence of clustering, but also from a consideration of the temperature effect on the "critical microemulsion concentration", we argue that clustering in microemulsions with amphiphilic triblock-copolymer is favored by exothermic secondary aggregation. Concerning the cluster lifetime, the clusters in AOT microemulsions are highly dynamic and reshuffle permanently (probably on a time scale of a few microseconds) so that they cannot be detected as discrete aggregates by dynamic light scattering.[63] The clusters formed with amphiphilic triblock-copolymer, however, have a longer lifetime so that they appear separated from reverse micelles in the intensity autocorrelation functions.

Returning to the exchange and having a simple picture of surfactant L_2-microemulsions in mind, i.e., the dispersed aqueous pools are coated by a surfactant monolayer, it seems surprising that the migration of ionic solute is so slow even though large clusters are present. For droplet-type surfactant microemulsions usually a fusion−fission exchange mechanism is discussed.[28,50,54,55,68] In that model the droplets in contact open a pore in the separating monolayer, mix their aqueous contents and separate again. Both the energetics of monolayer bending and surfactant flipping as well as the droplet "stickiness" (in a dynamic view the lifetime of an droplet encounter pair) are supposed to determine the rate of exchange.[28,50,68] Since both k_{ex} and k_{cc} are so slow it is highly likely that the exchange mechanism in triblock-copolymer microemulsions is different from fusion−fission. It appears rather that the transport of charge carriers is efficiently hampered. Two possible reasons for that may be considered. The first is the already discussed competition for hydration water reducing the ion mobility. The second reason may be due to the polymeric nature of the employed amphiphile, which can sterically shield the reverse micelles, also in the clustered state. In these ways, the exchange facilitating effect of clusters is counteracted energetically and sterically. In view of that it appears questionable whether the concept of bending energy is applicable to microemulsions with amphiphilic triblock-copolymer. These, for all the discussed reasons, should be considered as their own class with respect to the distinction between nonionic and ionic microemulsions.

In summary, the attractive interactions among reverse micelles leading to clustering govern a variety of physical properties. This cannot be inferred from studies on the phase behavior or application of single methods. We emphasize that for a reliable picture of the complex liquids both static and dynamic properties have to be considered, at best covering a wide range of experimental time scale for a complete understanding.

Conclusions

L_2-microemulsions with the amphiphilic triblock-copolymer $EO_{13}PO_{30}EO_{13}$ (Pluronic L64) have been characterized by a variety of dynamic methods. The investigated microemulsion parameters are temperature and water content. The amphiphile

behaves in some aspects such as a typical nonionic surfactant. However, more differences with respect to standard surfactants appear, e.g., from a comparison of the exchange rate constants, which are throughout much smaller than those from standard systems. Also the mechanism responsible for electrical percolation and the strong viscosity increase when lowering the temperature is different: it is neither a transition from water-swollen reverse micelles into a bicontinuous structure nor entropically favored clustering. It is shown with pure microemulsions for the first time that a gradual clustering leads to network formation when lowering the temperature. The clustering is mediated via the two hydrophilic chains of the triblock-copolymer and is suggested to be an exothermic process. This is related to the strong temperature dependence of the so-called critical microemulsion concentration and reflecting temperature-induced changes in the solvent quality for $EO_{13}PO_{30}EO_{13}$ of both *p*-xylene and water. Such linked reverse micelles have a long lifetime as compared to entropically favored clustering. More work needs to be done in order to quantify the energetic contributions involved in clustering, and to describe the cluster lifetimes by an appropriate model.

Acknowledgment. H.M. gratefully acknowledges financial support from DFG (Germany) and NFL (Sweden). We thank Prof. G. Ilgenfritz (University of Köln, Germany) for access to the conductometer, and G. Svensk (Uppsala) and S. Hvidt (University of Roskilde, Denmark) for performing viscosity measurements. W. Brown (Uppsala) and P. Alexandridis (Buffalo) are thanked for helpful discussions.

References and Notes

(1) Förster, S.; Zisenis, M.; Wenz, E.; Antonietti, M. *J. Chem. Phys*. **1996**, *104*, 9956.
(2) Linse, P. In *Amphiphilic Block Copolymers: Self-Assembly and Application*; Alexandridis, P., Lindman, B., Eds.; Elsevier: Amsterdam, submitted.
(3) Alexandridis, P. *Curr. Opin. Colloid Interface Sci*. **1996**, *1*, 490.
(4) Rodriguez, S. C.; Singer, E. J. *Surfactant Sci. Ser*. **1996**, *60*, 211.
(5) Dickinson, E.; Lorient, D. *Food Macromolecules and Colloids*. The Royal Society of Chemistry: Cambridge, 1995.
(6) Zalipsky, S. *Bioconjugate Chem*. **1995**, *6*, 150.
(7) Torchilin, V. P.; Trubetskoy, V. S.; Whiteman, K. R.; Caliceti, P.; Ferruti, P.; Veronese, F. M. *J. Pharm. Sci*. **1995**, *84*, 1049.
(8) Edens, M. W. *Surfactant Sci. Ser*. **1996**, *60*, 185; and references therein.
(9) Mura, J. L.; Riess, G. *Polym. Adv. Technol*. **1995**, *6*, 497.
(10) Förster, S.; Antonietti, M. *Adv. Mater*. **1998**, *10*, 195.
(11) Caruso, R. A.; Giersig, M.; Willig, F.; Antonietti M. *Ber. Bunsen-Ges. Phys. Chem*. **1998**, *102*, 1540.
(12) Chander, S.; Polat, H.; Mohal, B. *Trans. Soc. Min. Metall. Explor*. **1995**, *296*, 55.
(13) Devanand, K.; Selser, J. C. *Macromolecules* **1991**, *24*, 5943.
(14) Alexandridis, P.; Andersson, K. *J. Colloid Interface Sci*. **1997**, *194*, 166.
(15) Alami, E.; Almgren, M.; Brown, W.; Francois, J. *Macromolecules* **1996**, *29*, 2229.
(16) Sandier, A.; Brown, W.; Mays, H.; Amiel, C. *Langmuir*, submitted for publication, 1999.
(17) Alami, E.; Almgren, M.; Brown, W. *Macromolecules* **1996**, *29*, 5026.
(18) Almgren, M.; Wang, K.; Asakawa, T. *Langmuir* **1997**, *13*, 4535.
(19) Meier, W.; Hotz, J.; Günther-Ausborn, S. *Langmuir* **1996**, *12*, 5028.
(20) Mays, H.; Almgren, M.; Dedinaite, A.; Claesson, P. M. *Langmuir*, in press.
(21) Johannsson, R.; Chassenieux, C.; Durand, D.; Nicolai, T.; Vanhoorne, P.; Jérôme, R. *Macromolecules* **1995**, *28*, 8504.
(22) Almgren, M.; Brown, W.; Hvidt, S. *Colloid Polym. Sci*. **1995**, *273*, 2.
(23) Chu, B.; Zhou, Z. *Surfactant Sci. Ser*. **1996**, *60*, 67.
(24) Mortensen, K. *Curr. Opin. Colloid Interface Sci*. **1998**, *3*, 12.
(25) Strey, R. *Colloid Polym. Sci*. **1994**, *272*, 1005.
(26) Chu, B. *Langmuir* **1995**, *11*, 414.
(27) Lindman, B.; Olsson, U. *Ber. Bunsen-Ges. Phys. Chem*. **1996**, *100*, 344.
(28) Mays, H. *J. Phys. Chem. B* **1997**, *101*, 10271.
(29) Alexandridis, P.; Olsson, U.; Lindman, B. *Macromolecules* **1995**, *28*, 7700.
(30) Alexandridis, P.; Olsson, U.; Lindman, B. *Langmuir* **1998**, *14*, 2627.
(31) Altinok, H.; Yu, G. E.; Nixon, K.; Gorry, P. A.; Attwood, D.; Booth, C. *Langmuir* **1997**, *13*, 5837.
(32) Goldmints, I.; Holzwarth, J. F.; Smith, K. A.; Hatton, A. T. *Langmuir* **1997**, *13*, 6130.
(33) Mays, H.; Almgren, M.; Brown, W.; Alexandridis, P. *Langmuir* **1998**, *14*, 723.
(34) Barreleiro, P. C. A.; Alexandridis, P. *J. Colloid Interface Sci*. **1998**, *206*, 357.
(35) Mays, H.; Almgren, M.; Brown, W. *Ber. Bunsen-Ges. Phys. Chem*. **1998**, *102*, 1648.
(36) Wu, G.; Chu, B. *Macromolecules* **1994**, *27*, 1766.
(37) Zhou, Z.; Hilfiker, R.; Hofmeier, U.; Eicke, H. F. *Prog. Colloid Polym. Sci*. **1992**, *89*, 66.
(38) Eicke, H. F.; Quellet, C.; Xu, G. *Colloids Surf*. **1989**, *36*, 97.
(39) Wu, G.; Zhou Z.; Chu, B. *Macromolecules* **1993**, *26*, 2117.
(40) Barreleiro, P. C. A.; Andersson, K.; Håkansson, B.; Olsson, U.; Alexandridis, P., submitted.
(41) Barela, T. D.; Sherry, A. D. *Anal. Biochem*. **1976**, *71*, 351.
(42) Schillén, K.; Brown, W.; Johnsen, R. M. *Macromolecules* **1994**, *27*, 4825.
(43) Provencher, S. W. *Computer Phys. Comm*. **1982**, *27*, 213.
(44) Eicke, H. F.; Borkovec, M.; Das-Gupta, B. *J. Phys. Chem*. **1989**, *93*, 314.
(45) Kahlweit, M.; Busse, G.; Winkler, J. *J. Chem. Phys*. **1993**, *99*, 5605.
(46) Mays, H.; Pochert, J.; Ilgenfritz, G. *Langmuir* **1995**, *11*, 4347.
(47) Lipgens, S.; Schübel, D.; Schlicht, L.; Spilgies, J. H.; Ilgenfritz, G. *Langmuir* **1998**, *14*, 1041.
(48) Lang, J.; Jada, A.; Malliaris, A. *Phys. Chem*. **1988**, *92*, 1946.
(49) Alexandridis, P.; Holzwarth, J. F.; Hatton, T. A. *J. Phys. Chem*. **1995**, *99*, 8222.
(50) Mays, H.; Ilgenfritz, G. *J. Chem. Soc., Faraday Trans*. **1996**, *92*, 3145.
(51) Ponton, A.; Bose, T. K.; Delbos, G. *J. Chem. Phys*. **1991**, *94*, 6879.
(52) Kahlweit, M.; Strey, R.; Busse, G. *J. Phys. Chem*. **1990**, *94*, 3881.
(53) Lemaire, B.; Bothorel, P.; Roux, D. *J. Phys. Chem*. **1983**, *87*, 1023.
(54) Almgen, M.; Johannsson, R. *J. Phys. Chem*. **1992**, *96*, 9512.
(55) Almgren, M.; Mays, H. In *Handbook of Microemulsion Science and Technology*; Kumar, P., Mittal, M., Eds.; Marcel Dekker: New York, 1999.
(56) Infelta, P. P.; Grätzel, M.; Thomas, J. K. *J. Phys. Chem*. **1974**, *78*, 190.
(57) Tachiya, M. Chem. *Phys. Lett*. **1975**, *33*, 289.
(58) Vasilescu, M.; Caragheorgheopol, A.; Almgren, M.; Brown, W.; Alsins, J.; Johannsson, R. *Langmuir* **1995**, *11*, 2893.
(59) Atik, S. S.; Thomas, J. K. *J. Am. Chem. Soc*. **1981**, *103*, 3543.
(60) Smoluchowski, M. V. *Z. Phys. Chem*. **1917**, *92*, 129.
(61) Armstrong, J. K.; Parsonage, J.; Chowdhry, B.; Leharne, S.; Mitchell, J.; Beezer, A.; Löhner, K.; Laggner, P. *J. Phys. Chem*. **1993**, *97*, 3904.
(62) Mays, H.; Mortensen, K.; Brown, W. Microemulsions Studied by Scattering Techniques. In *Scattering in Polymeric and Colloidal Systems*; Brown, W., Mortensen, K., Eds.; Gordon and Breach: Reading, U.K., 1999; in press.
(63) Mays, H. Unpublished results.
(64) Eshuis, A.; Mellema, J. *Colloid Polym. Sci*. **1984**, *262*, 159.
(65) Smeets, J.; Koper, G. J. M.; van der Ploeg, J. P. M.; Bedeaux, D. *Langmuir* **1994**, *10*, 1387.
(66) Schlicht, L.; Spilgies, J. H.; Runge, F.; Lipgens, S.; Boye, S.; Schübel, D.; Ilgenfritz, G. *Biophys. Chem*. **1996**, *58*, 39.
(67) Simha, R. *J. Appl. Phys*. **1952**, *23*, 1020.
(68) Fletcher, P. D. I.; Horsup, D. I. *J. Chem. Soc., Faraday Trans*. **1992**, *88*, 855.